Supporting Information

Hydrogels as Solid Supports for Enzyme Immobilization: Intrinsic Kinetics and Error Propagation

Hector D. Neira[a] & Amy E. Herr[a,b]

[a]UC Berkeley/UCSF Graduate Program in Bioengineering, [b]Department of Bioengineering, University of California Berkeley, Berkeley, CA 94720, United States

Table of Contents

Figure S1. Eliminating Signal from Adsorbed Alkaline Phosphatase.

We observed unexpected variability in the calculated reaction rates for the same substrate concentrations in early immobilized enzyme kinetics experiments. As the same gaskets were used for introduction of the enzyme into the gel and for kinetics measurements over the course of several experiments, we hypothesized that our immobilized enzyme kinetics measurements were confounded by activity of calf intestinal alkaline phosphatase (AP) adsorbed onto the gaskets. To test this hypothesis, we measured formation of fluorescent DiFMU in gel regions that were not exposed to AP and compared it to gel regions that were exposed to AP on the same gasket. 75 μM DiFMUP solutions were prepared in 100 mM Tris, 150 mM NaCl, 50 mM $MgCl_2$, 0.1 mM $ZnCl_2$ buffer titrated to pH 7.8 with HCl. As a negative control, we included a denaturing detergent (sodium dodecyl sulfate, SDS) in the reaction buffer in some wells on the same gasket. Formation of DiFMU upon dephosphorylation of DiFMUP was measured at 30 s intervals for 3 min in the gasket fixtures with the same instrument and measurement settings detailed in the main text. The rate of formation of fluorescent DiFMU in gel regions not exposed to AP was ~20% of the rate measured in regions containing AP, supporting our original hypothesis. To mitigate the effects from AP adsorbed on the gasket, we washed the gasket in a denaturing, reducing buffer at 55°C for 1 hr.[1] After the stringent wash, the gasket fixture was reassembled on bare glass (no gel) and fresh solutions of DifMUP were added. The stringent wash protocol practically eliminated formation of fluorescent DiFMU due to adsorbed AP.

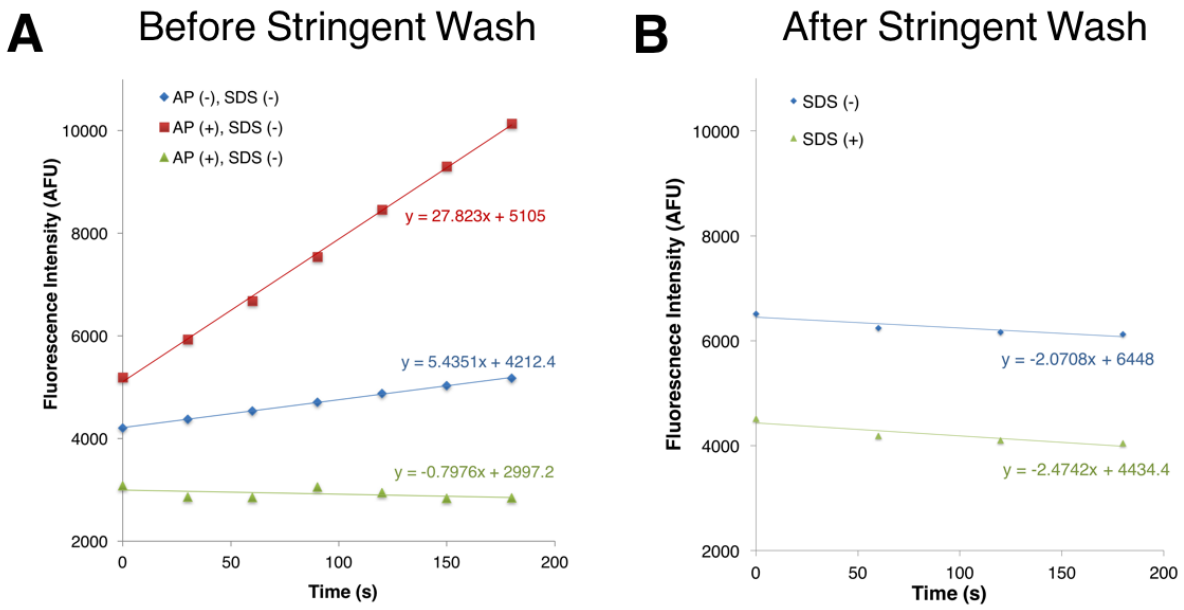

Figure S1. Stringent gasket wash conditions reduce variability in kinetics measurements. (A) Formation of fluorescent products upon dephosphorylation of DiFMUP were observed in hydrogel regions that were never exposed to AP at a rate ~ 20% of the rate of hydrogel regions containing 1.7nM AP. (B) Formation of fluorescent product due to adsorbed AP was practically eliminated after washing the gaskets in 0.5 M Tris-HCl pH 6.8, SDS (2% w/v), 2-mercaptoethanol (0.8% v/v) buffer at 55°C for ~1 hr[1] prior to starting time course measurements to inactivate or remove AP adsorbed to the gasket. Post-wash measurements were made after reassembling the gasket fixture on bare glass (no gel). AP(-) = gel region never exposed to AP, AP (+) = gel region with immobilized AP, SDS (-) = reaction buffer does not include SDS, and SDS (+) = reaction buffer includes SDS.

Figure S2. Controlling Immobilized Enzyme Concentration

We introduced the enzyme into the benzophenone-modified polyacrylamide (BPMA-PA) gels by placing a concentrated solution of enzyme over a gel and allowing the system to equilibrate by diffusion. The final, immobilized enzyme concentration, [$C_{immobilized}$], is reduced from the bulk enzyme concentration owing to: thermodynamic partitioning[2] that excludes enzyme from entering the gel and the efficiency of covalent attachment of enzyme to the gel, η_{imm}.[3,4,5] Prior to immobilization, partitioning of the macromolecules into the gel matrix imposes an upper limit on the concentration of enzyme in the gel, [C_{gel}], at equilibrium. The ratio of [C_{gel}] to the nominal solution concentration, [C_o], applied over the gel is the partition coefficient ($K_{partition} = \frac{[C_{gel}]}{[C_o]}$). $K_{partition}$ is expected to be < 1.0 for macromolecules such as AP (MW ≈ 140kDa);[2] and thus, the in-gel protein-mass available for covalent immobilization is < [C_o]. We define η_{imm} as the fraction of [C_{gel}] retained in the gel after photoactivated, covalent attachment and removal of unbound protein. Our group has previously reported η_{imm} for proteins in BPMA-PA gels ranging from 1.8 to ≥ 97% in closed microfluidic devices,[3,4] and ~27% for open thin gel films such as the ones used in this study.[5] As η_{imm} < 1 are expected, only a fraction of [C_{gel}] is expected to covalently attach to BPMA-PA gels. We investigated the relationship [C_{gel}] and [$C_{immobilized}$]. [C_{gel}] is related to [C_o] by the partition coefficient. We introduced and immobilized Green Fluorescent Protein (GFP) into 6% T BPMA-PA gels at different [C_o] as described. To assess η_{imm}, we measured GFP fluorescence and calculated the ratio of mean fluorescence before and after washing unbound GFP (Figure S2A). The results suggest that η_{imm} remains approximately constant (~20%) as a function [C_o] (Figure S2B). Therefore, we conclude that adjusting [C_o] is sufficient to tune [$C_{immobilized}$]. Increasing [C_o] or decreasing the gel density (higher $K_{partition}$)[2] would yield concomitant increases in [$C_{immobilized}$] while the converse adjustments would cause a decrease in [$C_{immobilized}$]. Notably, lower [$C_{immobilized}$] may be desirable for enzymes with high catalytic activity as rapid consumption of the substrate at high [$C_{immobilized}$] may lead to mass transport limitations. For sparingly available enzymes, alternate loading methods not subject to the partitioning limit (e.g., matched-volume rehydration,[6] electrophoresis[7]) could minimize enzyme consumption while yielding the desired [$C_{immobilized}$]. Control over [$C_{immobilized}$] facilitates determination of the [$C_{immobilized}$] window that allows for enzyme kinetics measurements free of confounding mass transport limitations.

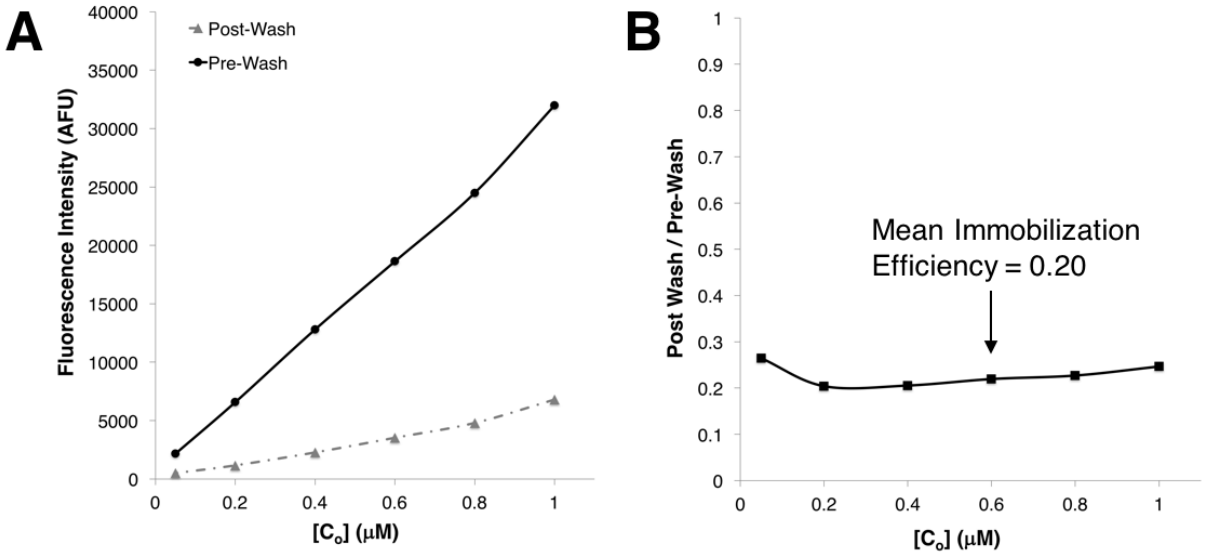

Figure S2. Immobilization efficiency of proteins in BPMA-PA gels is independent of nominal concentration of protein applied over the gel, [C_o]. (A) Fluorescence intensity of GFP post UV immobilization was measured before and after washing away unbound protein. (B) The ratio of GFP fluorescence after wash to GFP fluorescence before the wash quantifies immobilization efficiency (η_{imm}), which remained approximately constant for all [C_o] tested.

Figure S3. Kinetics of Alkaline Phosphatase in Solution

For control experiments with free AP, formation of DiFMU upon dephosphorylation of DiFMUP was measured at 15 s intervals for 3 min in a black, flat bottom 96-well plate (Corning) with the same instrument and measurement settings detailed in the main text. DiFMUP solutions were prepared in 100 mM Tris, 150 mM NaCl, 50 mM $MgCl_2$, 0.1 mM $ZnCl_2$ buffer titrated to pH 7.8 with HCl and loaded on individual wells (n = 4 per concentration). AP was then added to individual wells to a final concentration of 0.232 nM (0.464 nM catalytic site concentration as AP is a dimeric enzyme), and immediately loaded on the instrument for fluorescence time course measurements at room temperature. To generate the fluorescent product calibration curve, fluorescence of DiFMU solutions prepared in the indicated buffer was measured in individual wells (n = 4 solutions per concentration). Estimated K_m, V_{max}, and k_{cat} are summarized in Table 1 in the main text.

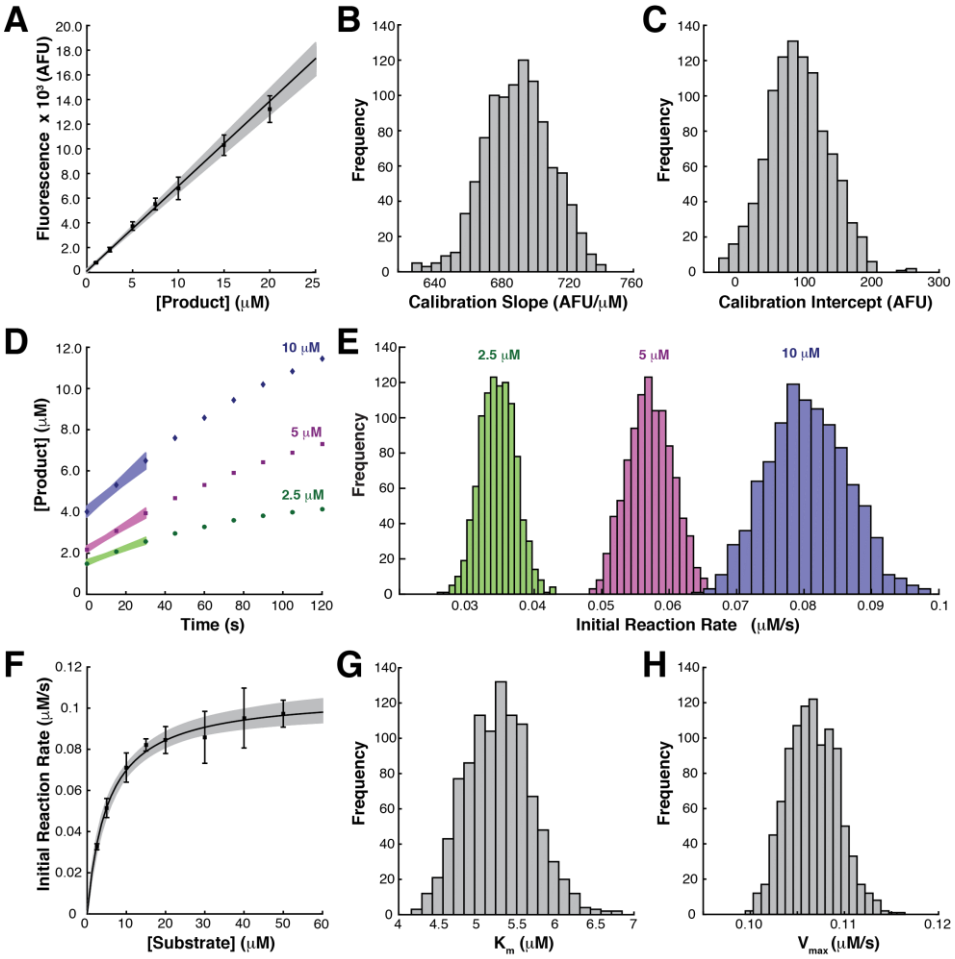

Figure S3. Kinetics of alkaline phosphatase in solution with propagated error through in all data manipulation steps. (A) Product calibration curve (black line) constructed from mean calibration slope and intercept of bootstrap samples overlaid with all possible calibration curves from bootstrap procedure (gray lines) and means of original calibration data (■, n = 4 per concentration). (B, C) Distributions of product calibration parameters from bootstrap procedure. (D) Representative calibration-corrected time course data sets from gel regions exposed to (●) 2.5, (■) 5, and (♦) 10 □M DiFMUP solutions overlaid with all possible linear fits from bootstrap calibration-corrected time course data sets yielded distributions of initial reaction rates (E) extracted from the slope term of the linear fits from all bootstrap calibration-corrected time course data sets. (F) MM curve (black line) constructed from mean calibration K_m and V_{max} parameters from all initial reaction rate bootstrap samples overlaid with all MM curves from bootstrap procedure (gray lines) and mean initial reaction rates (■, n = 4 initial reaction rate measurements per concentration). (G, H) Distributions of MM model parameters from bootstrap procedure. All error bars represent one standard deviation of the mean.

Extended Bootstrapping Methods

A bootstrapping method to propagate uncertainty in the product calibration data onto the final estimates K_m, V_{max}, and k_{cat} and respective uncertainties was developed. An adaptation of the bootstrapping method for controlled experiments described by Jones *et al.*[8,9] is presented. The approach was implemented in three stages: (i) calibration correction, (ii) initial reaction rate calculation, and (iii) fitting the Michaelis-Menten model. All bootstrap samples were constructed from 1000 iterations of sampling with replacement.

(i) Calibration Correction: A product fluorescence calibration curve determined as detailed in the main text, and the residuals normalized to their respective concentration. The normalized residuals were multiplied by a constant factor:

$$\sqrt{\frac{n}{n-p}} \quad (1)$$

where n is the number of measurements in the calibration curve and p is the number of parameters in the regression model. Bootstrap samples of the same size as the original calibration data set were generated from the pool of adjusted normalized residuals by sampling with replacement. Corresponding bootstrap samples of product fluorescence were calculated as

$$f = mx + b + xR^* \quad (2)$$

where f is the estimated fluorescence response for each adjusted normalized residual (R^*), and m and b are the slope and intercept from the original product fluorescence calibration curve, respectively. A new calibration curve was generated from each bootstrap sample of product fluorescence yielding a set of bootstrap calibration curves ($y_i^* = m_i^*x + b_i^*$), where i is the index of the bootstrap sample of product fluorescence utilized to generate the i^{th} calibration curve.

For illustration, we present truncated data sets for the in-solution enzyme kinetics measurements presented above (Schemes S1 and S2). The calibration curve (y = 688.8x + 91.62, n = 28 measurements, p = 2 parameters, Figure S3A) from the original calibration data set was utilized to construct bootstrap samples from the pool of R^*. Note that some R^* values are repeated multiple times in a bootstrap sample due to random sampling with replacement (Scheme S1). Where appropriate, R^* values have been color coded to show correspondence between bootstrap samples and the original pool of R^* (Scheme S1). This process produced a distribution of calibration slopes and intercepts (Figure S3A – S3C), which were then applied to each fluorescence time course measurement producing a set of calibration-corrected time course data sets (Scheme S2).

(ii) Initial Reaction Rate Calculation: Bootstrap samples of calibration-corrected time course data were generated by sampling with replacement from all the possible calibration-corrected values for each time point (Scheme S2). The initial reaction rate for each bootstrap sample of calibration-corrected time course data was determined by linear regression producing a distribution of initial reaction rate values from each set of original fluorescence time course measurements (Scheme S2, Figure S3D and S3E).

(iii) Fitting the Michaelis-Menten Model: The last stage of the error propagation process mirrors the calibration correction process (Scheme S1). The mean and residuals from the mean initial reaction rate value (R_m) for each set of fluorescence time course measurements were calculated. The Michaelis-Menten model was then fitted to the mean initial reaction rates providing $K_{m\text{-}initial}$ and $V_{max\text{-}initial}$ estimates. R_m values were adjusted according to Equation 1, where n was the number of original fluorescence time course measurements (n = 64) and p was the number of parameters in the Michaelis-Menten model (p =2) resulting in a pool of adjusted R_m values (R^*_m). Bootstrap samples of the same size as the original number of fluorescence time course measurements were generated from the pool of R^*_m. Corresponding bootstrap samples of initial reaction rates were calculated as

$$v([S])^* = \frac{V_{max-initial}[S]}{K_{m-initial}+[S]} + R_m^* \quad (3)$$

where $v([S])^*$ is the estimated initial reaction rate as a function of the substrate concentration used for the original fluorescence time course measurement estimated from the value of R^*_m. The Michaelis-Menten model was fitted to each bootstrap sample of $v([S])^*$ values generating distributions of $K^*_{m\text{-}j}$ and $V^*_{max\text{-}j}$ values, where j is the index of the bootstrap sample of $v([S])^*$values utilized to generate the j^{th} set of

parameter estimates (Figure S3F – S3H). The uncertainty in each term is reported as one standard deviation from the mean the distributions of $K^*_{m\text{-}j}$ and $V^*_{max\text{-}j}$.

Scheme S1. Overview of bootstrap calibration process. The same process is applicable to the Michaelis-Menten fitting stage. Truncated calibration data is shown.

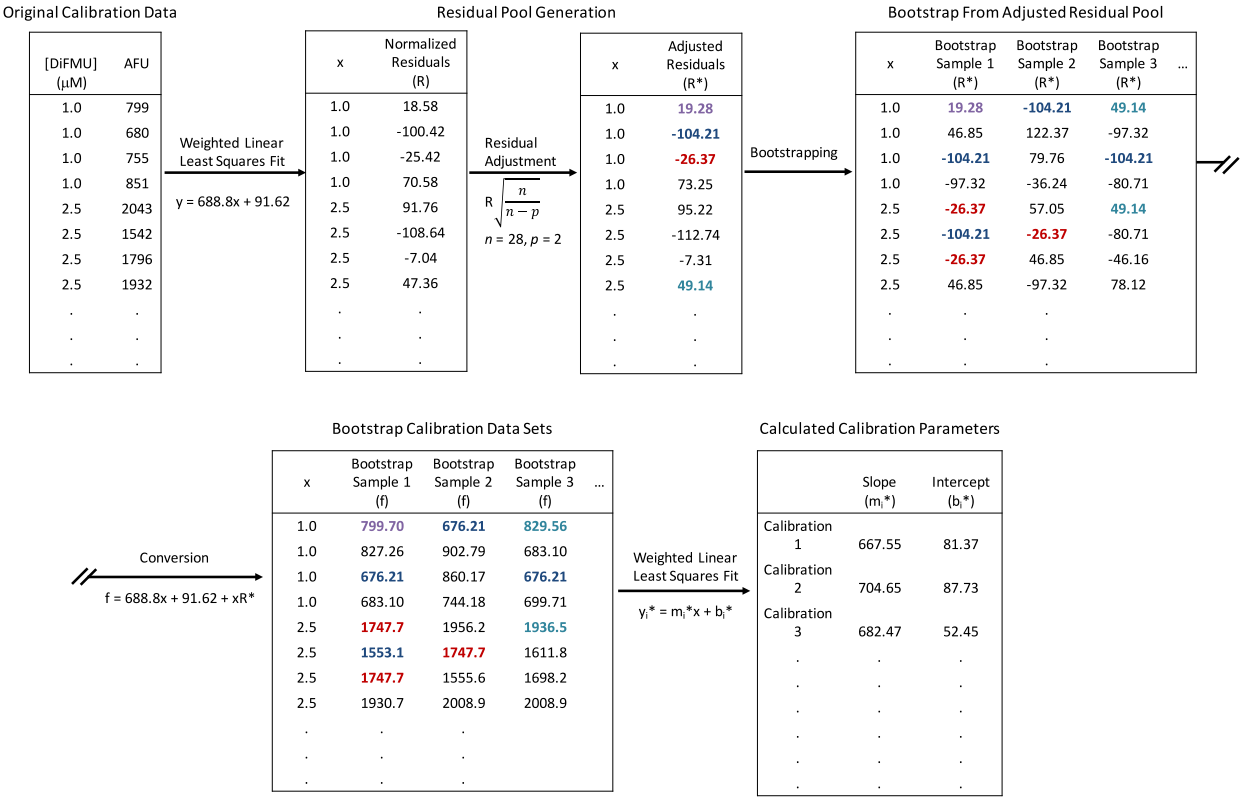

Scheme S2. Calibration correction process and initial reaction rate calculation. Truncated data set at 2.5mM DiFMUP concentration is shown.

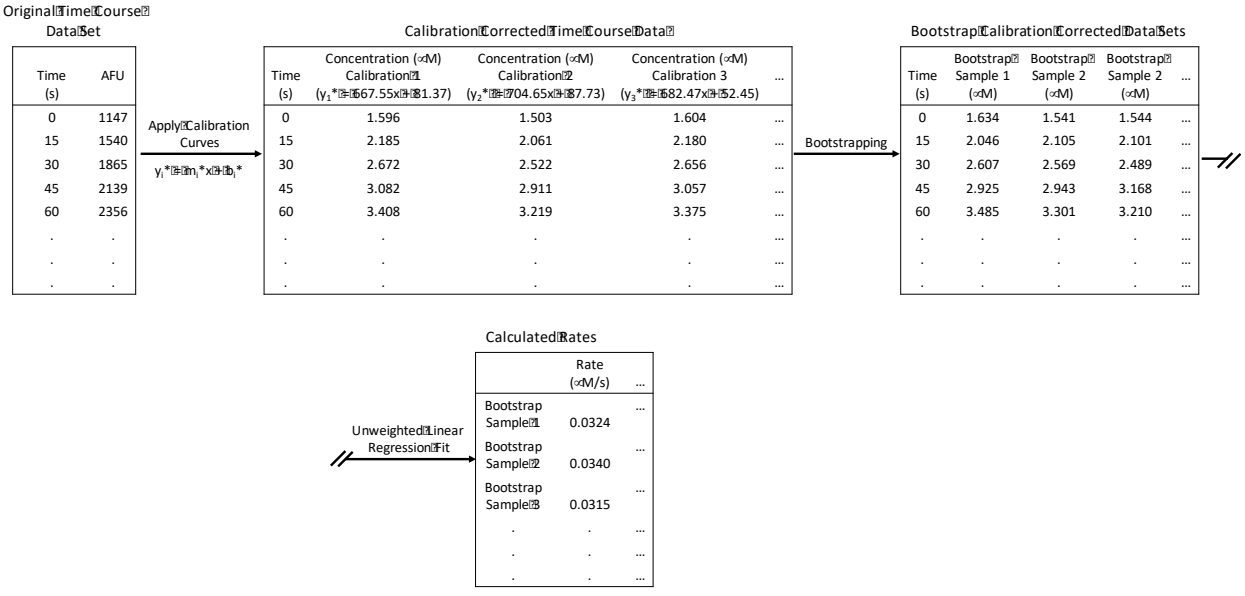

SI References:

(1) Kang, C.-C.; Yamauchi, K. A.; Vlassakis, J.; Sinkala, E.; Duncombe, T. A.; Herr, A. E. *Nat. Protoc.* **2016**, *11* (8), 1508–1530.
(2) Tong, J.; Anderson, J. L. *Biophys. J.* **1996**, *70*, 1505–1513.
(3) Hughes, A. J.; Lin, R. K. C.; Peehl, D. M.; Herr, A. E. *Proc. Natl. Acad. Sci. U. S. A.* **2012**, *109* (16), 5972–5977.
(4) Hughes, A. J.; Herr, A. E. *Proc. Natl. Acad. Sci. U. S. A.* **2012**, *109* (52), 21450–21455.
(5) Hughes, A. J.; Spelke, D. P.; Xu, Z.; Kang, C.-C.; Schaffer, D. V; Herr, A. E. *Nat. Methods* **2014**, *11* (7), 749–755.
(6) Vlassakis, J.; Herr, A. E. *Anal. Chem.* **2015**, *87*, 11030–11038.
(7) Yeh, C. Investigation of Electrophoretic Loading and Enhanced Mechanical Properties of Hydrogels for Delivery of Therapeutic Proteins, The Queensland University of Technology, 2010.
(8) Jones, G.; Wortberg, M.; Kreissig, S. B.; Hammock, B. D.; Rocke, D. M. *Anal. Chem.* **1996**, *68* (5), 763–770.
(9) Jones, G.; Rocke, D. M. *Technometrics* **1996**, *41* (3), 224–233.